LBL-37833
UC-400

Lawrence Berkeley Laboratory
UNIVERSITY OF CALIFORNIA

ENERGY & ENVIRONMENT
DIVISION

To be presented at the Western States Section of the
Combustion Institute, Stanford, CA, October 31, 1995,
and to be published in the Proceedings

Effects of Buoyancy on Premixed Flame Stabilization

B. Bédat and R.K. Cheng

October 1995

ENERGY
AND ENVIRONMENT
DIVISION

Prepared for the U.S. Department of Energy under Contract Number DE-AC03-76SF00098

LBL-37833
UC-400

Effects of Buoyancy on Premixed Flame Stabilization

Benoit Bédat and Robert K. Cheng

Energy and Environment Division
Lawrence Berkeley National Laboratory
University of California
Berkeley, California 94720

October 1995

This work was supported by NASA Microgravity Sciences and Applications Division and NASA Lewis Research Center under Contract No. C-32000-R through the U.S. Department of Energy under Contract No. DE-AC03-76SF00098.

EFFECTS OF BUOYANCY ON PREMIXED FLAME STABILIZATION

Benoit Bédat and Robert K. Cheng

Combustion Group
Energy & Environment Division
Lawrence Berkeley National Laboratory
Berkeley, CA 94720

Abstract

The stabilization limits of v-flame and conical flames are investigated in normal gravity (+g) and reversed gravity (up-side-down burner, -g) to compare with observations of flame stabilization during microgravity experiments. The results show that buoyancy has most influence on the stabilization of laminar V-flames. Under turbulent conditions, the effects are less significant. For conical flames stabilized with a ring, the stabilization domain of the +g and -g cases are not significantly different. Under reversed gravity, both laminar v-flames and conical flames show flame behaviors that were also found in microgravity. The v-flames reattached to the rim and the conical flame assumed a top-hat shape. One of the special cases of -g conical flame is the buoyancy stabilized laminar flat flame that is detached from the burner. These flame implies a balance between the flow momentum and buoyant forces. The stretch rates of these flames are sufficiently low ($< 20\ s^{-1}$) such that the displacement speeds S_L are almost equal to the laminar burning speed S_L^0. An analysis based on evaluating the Richardson number is used to determine the relevant parameters that describe the buoyancy/momentum balance. A perfect balance i.e. $Ri = 1$ can be attained when the effect of heat loss from the flame zone is low. For the weaker lean cases, our assumption of adiabaticity tends to overestimate the real flame temperature. This interesting low stretch laminar flame configuration can be useful for fundamental studies of combustion chemistry.

INTRODUCTION

Our recent studies [1,2] of laminar and turbulent premixed conical flames subjected to normal gravity (+g), reversed gravity (upside-down flame, -g) and microgravity (μg) have demonstrated that buoyancy affects many aspects of flame propagation. In normal gravity, the most noticeable effect is buoyancy-induced flame flickering. The pulsating flame motion has a distinct characteristic frequency and generates flow fluctuations throughout the entire flowfield. Flames in -g and μg are not influenced by buoyancy driven instabilities. Their general flame features such as flame cone height, however, are not always consistent with those of normal gravity flames [2]. For example, the different flame cone heights for +g, -g and μg do not converge with increase flow rate. Therefore, the effects of buoyancy seem to persist even at higher momentum. This trend is contrary to the notion that buoyancy effects would diminished with increase flow momentum. These differences would present obstacles in merging experiments with theoretical analyses that do not include the buoyancy effects [e.g. 3]. To support the development of theories that can consider flame/buoyancy coupling, our goal is to characterize, experimentally, the overall features and flowfield of +g, -g and μg flames. The study of μg flames is the key to our strategy to provide the link between the sometimes counter-intuitive trends shown by the +g and -g flames. This will help to establish empirical criteria or limits for estimating the influence of buoyancy on open premixed flames.

Our first impression of μg flames is that they are difficult to ignite and stabilize. Robust burning flames in normal gravity can blow-off when μg is reached. This had occurred in both drop tower experiments and parabolic flights. Attempts to ignite in μg were not always successful. Due to a lack of knowledge on how buoyancy influences flame stabilization processes, we had little confidence in choosing the appropriate conditions for μg experiments. The purpose of this paper is to rectify the situation by determining the stabilization limits of +g and -g flames to obtain better guidance to our future μg experiments. A complete study should of course also include the determination of the stabilization

limits in μg. Unfortunately, such a study is not presently feasible as the experiments require many drop tower runs and/or flight parabolas.

The two flame configuration used for our work are conical flames [1,2] and rod-stabilized v-flames [4]. Conical Bunsen flames are stabilized at the rim or by a ring fitted within the burner exit. The v-flames are stabilized by a 2 mm rod placed across the center of the burner exit. Flash-back and blow-off limits are obtained under both laminar and turbulent flow conditions.

During the course of our investigation of -g flames, we discovered the existence of buoyancy stabilized laminar flames. These flames are very stable, relatively flat, and completely detached from the burner. Their stabilization mechanism does not rely on flow attachment at a flame holder or at the burner rim nor requires external means such as stagnation plate [5] or swirl [6] to produce a divergence flowfield. The basic implication is that buoyancy in the hot products induces the appropriate flowfield that enables the flame to propagate steadily into the reactants stream coming out of the burner.

This unique flame configuration is of fundamental importance to characterize flame/buoyancy coupling because it encapsulates the essential physics of the problem. As shown by our previous LDA measurements, the main difference between +g and -g conical flames is in the flow divergence of products regions. The effects downstream of the flame zones affect the mean flame features upstream primarily through changes in the mean pressure field. This seems to be the important mechanism through which buoyancy influences premixed flame propagation. Here, the effects of buoyancy is dominant because all other effects associated with flame geometry and means of stabilization are absent. Therefore, this unique flame configuration is ideal for investigating how buoyancy interacts with flame generated flow momentum, what effects it has on the flowfield, and what are the relevant parameters to describe the interacting processes. Such knowledge would be very useful for analyzing the effects of buoyancy on more complex laminar and turbulent flames. Towards this aim, we carried-out a detail study of these buoyancy stabilized flat flames. First, the conditions under which they can be generated were determined. Next laser Doppler anemometry was used to measure the 2-D velocities in the flowfields. These velocity data were used in an analysis to characterize the buoyancy/flow balance in the flowfields.

EXPERIMENT AND DIAGNOSTICS

The schematic of the burner is shown in Figure 1. The burner has a 25 mm diameter circular outlet supplied by a converging nozzle fitted to a cylindrical settling chamber. The converging nozzle produces laminar flow with uniform velocity distribution. Turbulence is generated by placing a perforated plate place 16 mm upstream of the exit. The burner can be configured for two flame geometry. Conical flames are stabilized either at the rim or by a ring fitted inside the rim (insert A). The ring reduces the effective diameter of the burner outlet to 20.6 mm. The mean purpose for using this ring is that it stabilizes very lean flames. V-flames are stabilized by a rod of 2 mm diameter placed across the burner exit (insert B). The fuel (methane) and air are metered separately by two electronic flow controllers interfaced with a PC. For stabilization limits studies, the system is programmed to increase or decrease the equivalence ratio linearly while maintaining a constant flow rate. For the reversed gravity experiments, the burner is immersed in a cooling water bath to prevent pre-heating of the reactants and the flow rate of the cooling water is constant at about 3.5 liter per minute (insert C).

Laser schlieren is a convenient means to observe the changes in flame shape and is the principal diagnostic for mg experiments [1,2] . Our system employs a 0.5 mW He-Ne laser light and has a circular field of view of 75 mm. The schlieren stop is an opaque spot etched on a glass window. It produces a reverse field image (i.e., dark background), and regions of high density gradients appear bright. We use a CCD video cameras with high shutter speeds (up to 1/10000 sec) to capture the rapid changing flame structures. One innovation of our work is to exploit the interlace feature of standard video recording to double the recording rate from 30 to 60 Hz [1]. A two-component LDA system [4] is used to characterize the flowfields of buoyancy stabilized laminar flat flames. A 4-watt argon ion laser provides the laser source. The transmission optics is of conventional design with all four cross beams frequency shifted by Bragg cells. Differential shift of 2 MHz is used for both components and the co-validation criterion is 10 μs. The laser and transmission optics are mounted on a computer controlled traversing table to scan the flame automatically along fixed axis or to trace the flowline by feed-back control [7].

The experimental conditions cover flow rates, Q, from 0.2 to 0.9 liter/sec (mean velocity, U, of 0.5 to 2.0 m/s). The Reynolds numbers, Re, computed based on the exit diameter, D, are between 200 to 5500. Methane is use as

fuel with the equivalence ratio, ϕ, varied from 0.55 to 1.0. The turbulent intensity is less than 1% for the laminar flame and is 8% when the perforated plate is used. These conditions produce flame that are classified as wrinkle laminar flames [8].

RESULTS AND DISCUSSION

Flame Stabilization Limits

Flame stabilization limits for +g and -g v-flames are compared in Figures 2(a) and 2(b). The stable flame regions are bounded by the flash-back and blow-off limits at respectively high and low equivalence ratios. Also shown are the μg experimental conditions. They are all within the stable flame region prescribed by the limits of +g and -g flames. The laminar flame results in Figure 2(a) show that reversing the burner helps to stabilize leaner flames ($\phi < 0.6$). At Re = 2000, the blow-off limit is lowered from $\phi = 0.68$ in +g to about $\phi = 0.55$ in -g. This significant change in lean blow-off limit has important implication to design of practical applications. Many high-efficiency gas appliances have -g flames in that the burners are pointing down to the heat exchanger instead of the traditional heat-exchanger over burner configuration. The motivation for the up-side-down arrangement is to allow easy drainage of condensate when operating the system above 80% thermal efficiency. As our results demonstrated, the reversed burner allows stable burning of lean flames that emit lower concentrations of oxides of nitrogen. This design practice, therefore can also be exploited for lowering pollutant emissions.

We also observed that flash-back of laminar v-flames is preceded by the outer free edges of the two flame sheets attaching to the burner rim. This phenomenon is also observed in μg. Figure 3 shows two frames from a schlieren video for a μg experiment performed in drop tower. The initial conditions is close to the +g flash-back limit. Under normal gravity (Figure 3(a)), the two v-flame sheets are free to interact with ambient air. Transition to μg causes the right flame sheet to attach itself to the rim (Figure 3(b)). This is one of the few anecdotal evidence we have observed in μg that confirms the influence of buoyancy on μg flame stabilization. In the laboratory, both +g and -g flames form "M-flame" (both sheets attaching to the rim) prior to flash-back. For -g flames with lower flow rates (Re < 600) and close to the flash-back limit, center "V" branches of the M-flame open to the extent that the two flame sheets are almost horizontal. This interesting flame shape prompted us to explore and discover buoyancy stabilized flat flames.

The turbulent v-flames data of Fig. 2(b)) show that both +g and -g flames flash-back at equivalence ratios lower than those of laminar flames. This is a consequence of turbulence increasing flame speed such that under the same mean flow rate, a laminar flame remains stable and a turbulent flame may propagate up into the burner to cause flash-back. The differences between the +g and -g flash-back limits, however, are small compare to those shown in Fig. 2(a), and they convergence at Re > 2500. This shows that turbulent v-flame flash-back is not very sensitive to burner orientation. Another observation is that "M" shaped turbulent flames are never formed. The large fluctuations of the turbulent flame sheets edges as seen on the schileren videos may prevent this from occurring.

The corresponding turbulent blow-off limits for v-flames do not show significant differences between +g and -g conditions. This is in contrast to the large differences shown by the laminar flames. The main reason is that turbulence extends the stabilization limits of +g flames to much leaner equivalence ratios. Consequently, there is relative little difference between the +g and -g turbulence blows off limits. In view of these results that show a general lack of sensitivity to gravity, it is rather surprising that we encountered problems in stabilizing turbulent v-flames in μg. During our recent μg campaign on Learjet parabolic flights, only one of the chosen conditions ignited and propagated in mg. All the other conditions either failed to ignite or ceased to propagate after a few seconds. This demonstrate again that μg flame behavior is not easily predictable by laboratory experiments.

The stabilization domains for ring-stabilized conical flames are shown in Figures 4(a) for laminar cases, and 4(b) for turbulent cases. Compared to the v-flame, flash-back of both laminar and turbulent conical flames occur at much higher equivalence ratios. This is to be expected because the conical flame configuration supports very rich premixed flames and diffusion flames. As reported previously [2], the -g laminar conical flame tip is sometimes flattened by the buoyant hot products. This top-hat flame begins to appears close to flash-back limit. It is also observed in μg. Figure 5(a) and (b) are schlieren records showing that under identical flow and mixture conditions, gravitational level can effect the mean flame shapes. These top hat flames, however, are not observed under turbulent conditions. The wrinkled flame sheet seem to provide an extra degree of freedom to counteract the influence of buoyancy.

The blow-off limits show that reversed gravity tends to lower the blow-off limits for both laminar and turbulent flames. The improvement, however, are limited to conditions with low Re and the differences are much less that shown in Figure 2(a) for laminar v-flames. This can be attributed to the effectiveness of the ring stabilizer in generating stable conical flames under a wide range of condition. It is interesting to note that the μg turbulent conical flames experiments did not suffer from the same difficulties as the μg turbulent v-flames experiments. The broader stable region is one reason. The other may be that the conical flames are shielded by the hot products which help to buffer any transient perturbations that are unavoidable in μg facilities. This buffer zone however is absent in the v-flame configuration. Their flame sheets edges interact with ambient air. As shown by our schileren videos, flame movements originate from the edge can propagate upstream to the rod flame attachment region. These movements can de-stabilize flame attachment and lead to blow-off.

Buoyancy Stabilized Laminar Flat Flames

Stabilization Domain

In Figure 6, the conditions that support buoyancy stabilized detached laminar flat flames are shown against the stabilization limits of -g rim-stabilized laminar conical flames. The stable conical flame region is bounded by the blow-off limits, and two limits unique to this configuration. The new limits are respectively the limits for transitions to top-hat flames (similar to the one shown in Figure 5(b)), and inverted conical flame. The inverted conical flames are found under rich conditions where the top-hat flame evolve into a "W" shape flame with a cone formed in the center pointing back upstream. This flame cone sometimes disappear inside the burner and the conditions under which this situation occurs marks the upper limit.

The domain of detached flat flames occupy a small region at low Reynolds number centered at Re = 500 and $\phi \approx 0.7$. It is also possible to stabilize detached flames outside these boundaries. But the flames would not be very flat and may form a pronounced indentation at the center. A direct flame luminosity photograph (Figure 7) shows that the flame sits relatively close to the burner exit. As demonstrated in Figure 8 by a series of schlieren images for conditions covering the range of $300 < Re < 600$, the flame zones move away from the burner with increasing Re. The schlieren records also show the products/air interface located below the flame. The relative distance between the flame and the interface characterizes the thickness of the hot product layer that surrounds the flame zone. With increase Re, the thickness of the products zone also increases and the product/air interface becomes less apparent on the schlieren record. This fading suggests a reduction in the density gradient across this interface.

Velocity Measurements

The conditions chosen for detailed interrogation by LDA is listed in Table I. Figure 9 shows the 2D velocity vectors obtained for the case of Re = 557, $\phi = 0.725$. These flow vectors show clearly that buoyancy causes the flow in the products to stagnate and form a divergent flow region below the flame zone. The curved boundary outlined by the vectors is consistent with the shape of the product/air interface shown on schlieren. These results show that flow divergence in the product also causes flow divergence upstream in the reactants. This divergence effect seems to be the important flame stabilization mechanism. Divergence decelerates the flow issuing out of the burner. The flame then stabilizes itself at the position where the mean flow velocity equals its propagating speed. This is the same stabilization principle for stagnation point flames and weak swirl flames. The stretch rate, a, for the present configuration, defined by dU/dx or dV/dy, where U and V are the mean velocity in the axial, x, and radial, y, direction, is significantly lower. As shown in Figure 10, values of a deduced from dV/dy are less than 20 1/sec compared to 100 to 200 1/sec for stagnation plate stabilized flames and 25 to 50 1/sec for weak swirl stabilized flames. The mean stretch experienced by the buoyancy stabilized flat flame is even lower than those generated by flat-flame burners which is widely used for fundamental research on combustion chemistry.

The centerline velocity profile of Figure 11 shows that the velocity distribution is very similar to those of stagnation point flames. The origin of profile is the burner exit. Negative x and U represent, respectively, distance below the burner and downward velocity. Without the flame, the mean exit velocity is 0.54 m/s. With the flame, mean velocity decelerates to 0.3 m/s at x = -2 mm, which is the closest LDA measurement position possible. Flow deceleration continues until about $x = 4.5$ mm where a sharp rise in velocity signifies the flame region. The minimum velocity attained is considered as the flame speed S_L in accordance with the established flame speed definition for stagnation point flames and weak swirl flames. The acceleration through the flame zone reaches a maximum S_b. In the post-flame region, the linear deceleration represents buoyancy induced flow

divergence. The distance between the velocity maximum at the hot boundary of the flame zone, S_b, and the stagnation point where U is zero defines the product zone thickness at the centerline, d_b. The experimental values of S_L, S_b, and d_b are listed in Table I.

In Figure 12, the flame speed, S_L, deduced from the velocity profiles is compared with those obtained experimentally by Tseng et al [9] and numerically by Vagelopoulos et al [10]. Our data for Q > 0.15 l/s compare well with the measurements of Tseng et al [9] and the numerical results of Vagelopoulos et al [10]. It is interesting to note that the experimental data obtained by Vagelopoulos et al [10] obtained using counterflow twin flame burner are below their numerical predictions for lean mixtures. So they are in fact consistent with our measurements. The low stretch rates, a, determined for our flames suggest that our values of S_L are good approximations of S_L^0, the unstretched laminar burning velocity. The fact that our results are comparable to those determined by other methods (i.e. spherical flame [9], counterflow twin flame technique[10]) with negligible heat loss demonstrates that our flames with Q > 0.15 l/s are near adiabatic. Deviation of ours results for Q < 0.15 l/s from the prediction [10] can be explained by heat loss. Premixed flames are very sensitive to heat losses, a small amount of energy extracted from the flame front can modify its velocity [11]. For our flames the effects of heat loss is diminished with increasing the stand off distance, x_f, as defined in Figure 13. As seen in table 1 where values of x_f are shown. as the flame moves away from the burner and reduces its heat loss to the water bath, S_L for ϕ = 0.7, decreases from 10 to 16.4 cm/s, corresponding to a variation of about 40 %.

Analysis

The main difference between these flames and those stabilized in stagnation point flows is that the stretch rates in stagnation point flows are prescribed and maintained by external means such that the stretch rate can be adjusted independently by changing the mean flow velocity and/or the separating distance from the burner to the stagnation point. Except for high stretch situation where wall interaction or flame-to-flame interaction may become important, the overall flame behavior is generally predictable by numerical models because the important initial conditions such as stretch rate are conveniently defined. Our buoyancy stabilized flames, on the other hand, are self sustained. They are more difficult to model because of a lack of clearly defined initial and boundary conditions. From the velocity results, it appears that flow acceleration generated by flame and heat release coupled with buoyancy produce the appropriate flow divergence to support stable flame propagation. Therefore, the appropriate starting point of the analysis is to evaluate the balance between buoyancy forces and momentum forces in this system.

Previous investigation of buoyancy induced flame flickering frequency [2] shows that the Richardson number, Ri, is a convenient parameter to compare the buoyant to the convective forces in premixed flames[12].

$$\mathrm{Ri} = \left(\frac{u_g}{u_c}\right)^2 \qquad (1)$$

Here subscripts g and c correspond to gravity and convection respectively. u_g can be estimated by equation 2 for an infinite gas layer of density ρ and thickness Δx,

$$u_g = \left(g \times \frac{\Delta\rho}{\rho} \times \Delta x\right)^{1/2} \qquad (2)$$

with g, $\Delta\rho$, ρ and Δx representing gravity acceleration, difference in density, the density of the layer and a characteristic length scale respectively.

Figure 13 illustrates the relevant parameters that can be used to apply the above analysis to the present system. The driving force of the system is of course the buoyant product layer that is responsible for the stabilization mechanism. For this geometry, $\Delta\rho$ is ρ_∞-ρ_b and Δx is d_b. With $\rho_\infty = \rho_u$ and invoking the heat release ratio $\tau = \rho_u/\rho_b$-1 Equation (2) becomes :

$$u_g = \left(g \times \tau \times d_b\right)^{1/2} \qquad (3)$$

Stability of the burnt gas layer is essential to the overall flame stabilization mechanism. Therefore the buoyant forces represented by u_g must be balanced by the convective forces. The relevant convective velocity is S_b, that is the velocity of the burnt gas at the flame front. Equation (1) becomes :

$$\mathrm{Ri} = g \times \tau \times \frac{d_b}{S_b^2} \qquad (4)$$

Equation (4) shows that the ratio of buoyancy to convective momentum forces along the center of the system is proportional to gravity acceleration, heat release ratio τ and a characteristics length scale of the products layer (i.e. its thickness d_b) and the initial velocity S_b at the boundary.

Richardson number of unity implies a balance between the buoyant and the convective forces. For typical lean

CH_4/air premixed flames with $g = 9.81$ m/s^2, $\tau = 5$, $S_L = 0.15$ m/s and $S_b \approx (\tau+1)\, S_L$. For such a balance to exist along the centerline, d_b would be about 17 mm. This is the same order of magnitude shown by the velocity profiles of Figure 11. The values of Ri deduced from the velocity measurements are listed in Table I and are plotted in Figure 14 against x_f. It is clear that only flames with $\phi > 0.72$ attain $Ri = 1$. These are also the cases where the measured S_L are close to S_L^0. As discussed before these cases are close to adiabatic.

For cases with equivalence ratio lower than 0.72, heat losses has a strong effect due to their close proximity to the burner and that they are relatively weak flames. Consequently, their Ri are above one. As shown by Botha [11], heat losses affect both the burning velocity and the temperature of the burnt gas. The values of τ used to compute the Richardson number correspond to the adiabatic conditions, this assumption would overestimate the burnt gas temperature for cases with significant heat losses and causes the values of Ri to reach above one.

Because we maintained a constant cooling water flow rate (3.5 liter/sec) for all cases, the influence of heat losses would be disproportionally large for lean weaker flames. Weak flames (leaner equivalence ratio) are very sensitive to heat losses, as demonstrated by the fact that energy required to extinguish lean flame is quite smaller than the for richer flames [11]. This is consistent with our results of Figure 14 where the effect of heat loss (i.e. Ri >1) are found only for the leaner cases. These result also suggests that heat losses should also influence the stabilization limits of the detached flat flame. Changes in cooling water flow rates can shift the stabilization region

Our analysis has shown that the thickness of the product layer d_b is an important empirical parameter for characterizing the effects of buoyancy on premixed laminar flames. It would be useful to investigate if it is possible to estimate d_b.

The only relevant reference we found is by Turner [13]. The experiment was a heavy salt jet projected upwards in water tank. Turner found that the maximum height, z_m, that the jet can reach is proportional to the internal Froude number F:

$$F = \frac{z^m}{r_0} = U_0 \times \left(g \times \frac{\rho_1 - \rho_2}{\rho_1} \times r_0 \right)^{-1/2} \quad (5)$$

where r_0, U_0 are the initial radius and velocity of the jet respectively.

To link the Turner's jet initial conditions to ours, we assume that the flame that the flame produces a stream of radius R_F, with velocity S_b and density r_b. The radius of the flame can be expressed by $R\ (U_o/S_L)$ with R the radius of the initial burner.

$$\frac{d_b}{R_F} \propto S_b \times \left(g \frac{\rho_\infty - \rho_b}{\rho_b} R_F \right)^{-1/2} \quad (6)$$

The values of d_b are compared with the experimental values in Table I. Equation (6) gives satisfactory predictions of the thickness of the burned layer for the cases that are close to adiabatic. This result is encouraging because for most open flame, the flame zone are well away from the burner and free of heat loss effects. The estimation given by Eq (6) would therefore be useful to estimate if the buoyancy could have significant effect on the flame zone.

The low stretch rate shown by our velocity measurements also suggests that these buoyancy stabilized flat flames would be a useful configuration for fundamental studies of combustion chemistry. Other configurations (i.e. flat flame burner, stagnation flow burners) commonly used to test and evaluate chemical kinetic schemes have to be corrected for the effects of strain. As discussed earlier the measured flame speed are extrapolated to its unstrained value for comparison with predictions [9,10]. The low stretch rate of these flames stabilized by buoyancy are closest to this idealized unstrained laminar flame. They would provide the instrained scalar distributions i.e. temperature and species for comparison to theoretical analysis. Though we found that the flame zone is also influenced by heat transfer as in the case of flat flame burners, these effects are negligible when the flames are sufficiently far away from the burner. Furthermore, the work carried-out here used a water bath to keep the temperature of the burner constant. This arrangement tends to promote heat transfer. We believe heat transfer to the burner can be reduced significantly by using a ceramic heat shield made of the same material used in out previous study of turbulent stagnation flames [5]. With better insulation, the domain for buoyancy stabilized flame flames as shown in Figure 6 can be broadened to offer wider range of conditions required by fundamental works.

CONCLUSION

The stabilization limits of v-flame and conical flames are investigated in normal gravity (+g) and reversed gravity (up-side-down burner, -g) and compared with observation of flame stabilization during microgravity experiments conducted in drop tower and parabolic

flights. The results show that buoyancy has most influence on the stabilization of laminar V-flame. In reversed gravity the stabilization limit shifts toward the lean conditions, closer to the flammability limit. Under turbulent conditions, the effects are less significant. For conical flames stabilized with a ring, the stabilization domain of the +g and -g cases are not significantly different. Under reversed gravity, both laminar v-flames and conical flames show flame behaviors that were also found in microgravity experiments. The v-flames reattached to the rim and the conical flame assumed a top-hat shape. For conical flames stabilized at the burner rim, reversing the burner generated several distorted flame shapes.

One of the special cases of -g conical flame is the buoyancy stabilized laminar flat flame that is detached from the burner. These flame implies a balance between the flow momentum and buoyant forces. Detailed analysis of the flow field by two component LDA shows that the buoyant forces in the burned gas create a stagnation point dowstream from the flame zone and divert the flow around the inner part of the flame where the momentum forces are greater. The flame stabilization mechanism involves flow divergence induced by the hot product gas layer that also create a divergence in the reactant gas. The flame then stabilizes itself at the position where the mean flow velocity equals its propagating speed. The stretch rate created by buoyancy is sufficiently low ($< 20\ s^{-1}$) such that the displacement speed S_L is almost equal to the laminar burning speed S_L^0 for the cases where the adiabatic conditions are reached.

The analysis based on evaluating the Richardson number shows that the relevant parameters to describe the balance between buoyant forces and the momentum forces are the velocity of the gas at the hot boundary of the flame zone, the heat release ratio and the thickness of the buoyant product as defined by the distance from the flame zone to the downstream stagnation point. The result of this analysis shows that a perfect balance i.e. $Ri = 1$ can be attained when the effect of heat loss from the flame zone is low. For the weaker lean cases, our assumption of adiabaticity tends to overestimate the real flame temperature. This interesting flame configuration can be useful as an alternative burner to the flat flame burner for fundamental studies of combustion chemistry.

ACKNOWLEDGEMENT

This work is supported by NASA Microgravity Sciences and Applications Division. Technical support is provided by NASA Lewis Research Center under contract No. C-32000-R. Project Scientist is Dr. Renato Colantonio. The authors would like to thank Dr. I. G. Shepherd for valuable discussions and to acknowledge Mr. Gary Hubbard for writing the computer controlled and data reduction software

REFERENCES

1. Kostiuk, L. W., and Cheng, R. K., *Experiments in Fluids,18:*59-68 (1994).

2. Kostiuk, L. W., and Cheng, R. K., *Combustion and Flame, 102:*27-40 (1995)

3. Bray, K. N. C., Libby, P.A., and Moss, J. B., *Combustion and Flame 61:*87-102 (1985).

4. Cheng, R. K. and Ng., T. T., *Combustion and Flame, 52* , 185-202 (1983).

5. Cho, P., Law, C. K., Hertzberg, J. H. and Cheng, R. K., *21th Symposium (International) on Combustion,* p. 1493, The Combustion Institute (1986).

6. Chan, C. K., Lau, S. K., Chin, W. K., and Cheng R. K. *24th International Symposium on Combustion* , The Combustion Institute, Pittsburgh, PA, p. 511-518 (1992).

7. Cheng, R. K., Shepherd, I. G., and Talbot, L., *22nd International Symposium on Combustion,* The Combustion Institute p. 771 (1988).

8. Borghi, R. *Recent Advances in the Aerospace Sciences.* Editor : Forradi Casci, Plenum, 117-138, (1985).

9. Tseng, L.K., Ismail, M.A. and Faeth, G.M., *Combustion and Flame* 95 : 410-426 (1993)

10. Vagelopoulos C.M. and Egolfopoulos F.N. and C.K. Law, *25th International Symposium on Combustion* , The Combustion Institute, p. 1341 Pittsburgh, PA, (1994).

11. Botha, J.P. and Spalding D.B., *Proc. Roy. Soc. (London),* A225 : 71-96 (1954)

12. Faeth, G.M. and Law, C.K. *Prog. Energy Combust. Scie.*20 : 65-119 (1994)

13. Turner, J.S., Buoyancy Effects in Fluids, Cambridge University Pess, (1973)

Table I

Q [l/s]	Re	ϕ	SL [m/s]	Sb [m/s]	db[(1)] [mm]	db[(2)] [mm]	xf [mm]	Ri[(3)]
0.09	264	0.70	0.11	0.34	8.9	5.6	-4.8	3.9
0.09	264	0.70	0.10	0.35	8.3	5.7	-4.8	3.5
0.11	323	0.70	0.12	0.48	9.3	7.9	-6.3	2.1
0.11	323	0.72	0.14	0.55	11.2	8.8	-4.3	2.0
0.13	380	0.70	0.14	0.53	10.2	8.9	-7.8	1.8
0.13	380	0.71	0.14	0.58	11.5	9.7	-6.0	1.7
0.15	440	0.70	0.16	0.69	15.0	11.6	-5.1	1.6
0.15	440	0.71	0.16	0.67	12.5	11.3	-7.5	1.4
0.15	440	0.72	0.17	0.74	13.5	12.3	-5.5	1.3
0.17	500	0.71	0.18	0.75	13.0	12.7	-8.5	1.2
0.17	500	0.72	0.19	0.83	14.4	13.8	-6.5	1.1
0.17	500	0.73	0.19	0.88	15.0	14.6	-5.8	1.0
0.17	500	0.74	0.19	0.90	16.1	14.8	-4.9	1.0
0.19	557	0.74	0.20	0.93	16.6	15.5	-7.5	1.0

(1) determined experimentally, (2)from Equation (6), (3) from Equation (4)

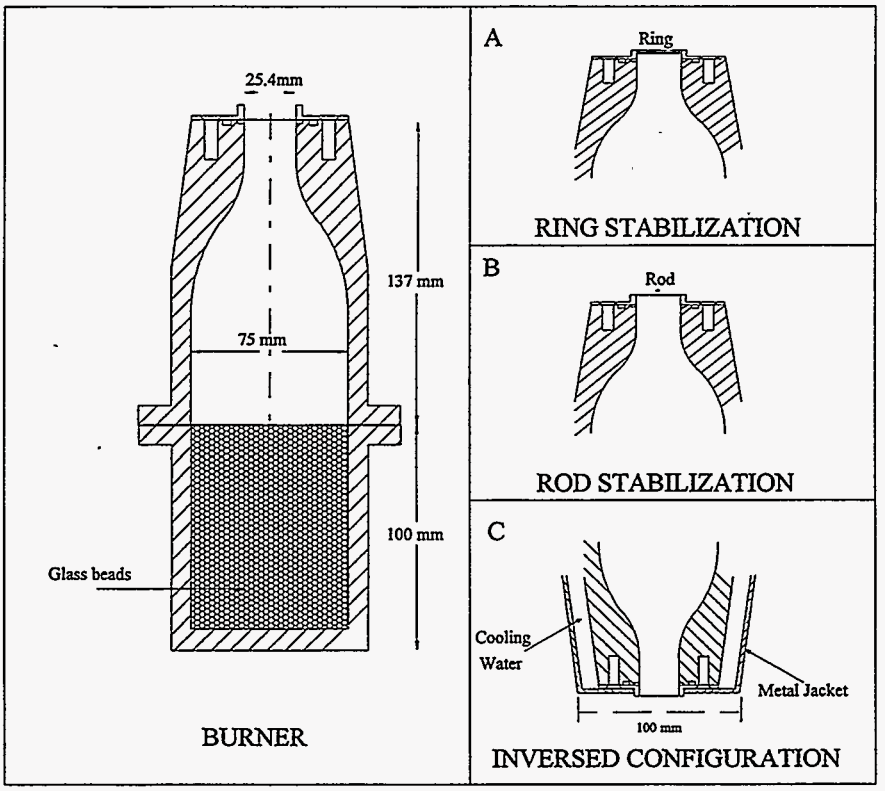

Figure 1 : Schematics of the burner.

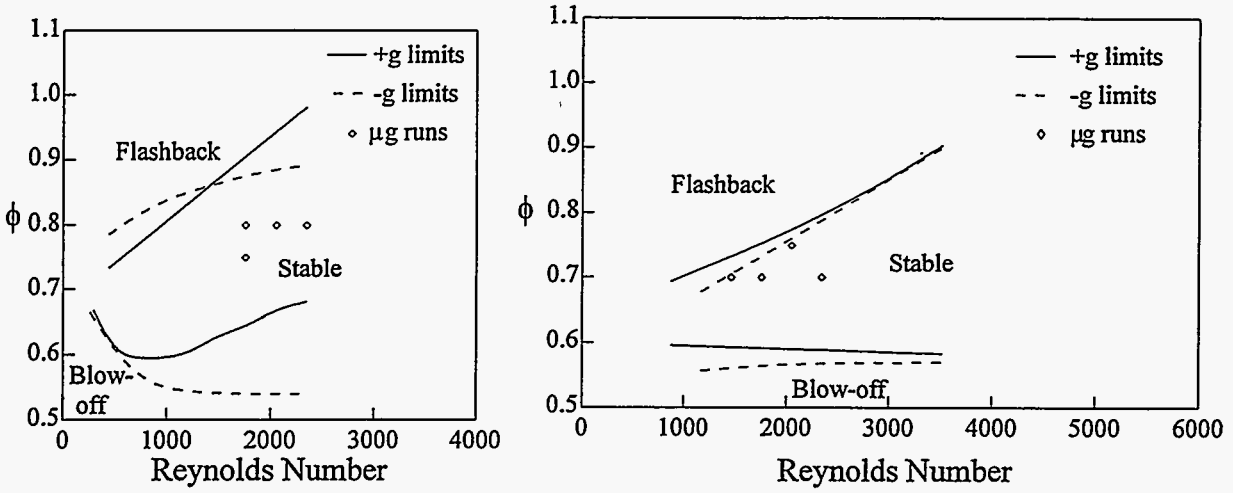

Figure 2 Blow-off and Flash-back limits for (a) laminar v-flames and (b) turbulent v-flames

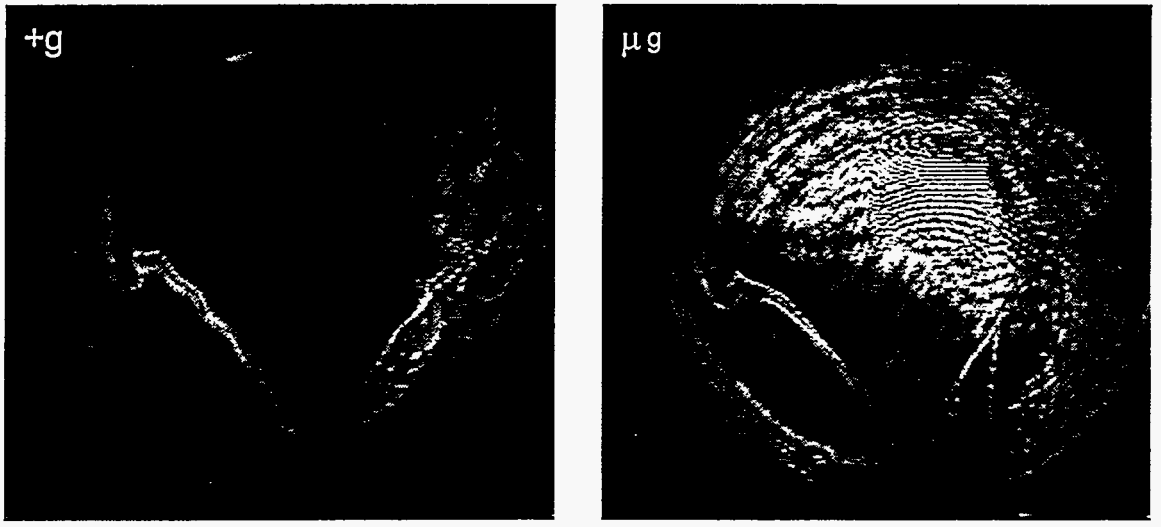

Figure 3 : Schlieren records of a µg laminar V-flame showing changes in flame shape from normal gravity (+g) and microgravity (µg).

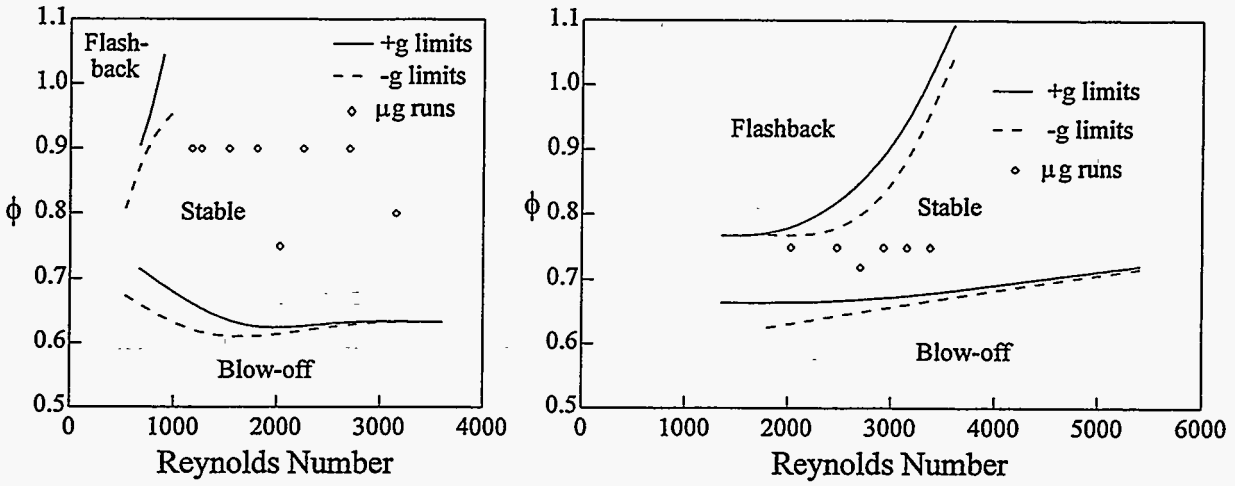

Figure 4 Blow-off and Flash-back limits for (a) laminar conical flames stabilized by the ring and (b) blow-off and Flash-back limits for turbulent conical flames stabilized by the ring

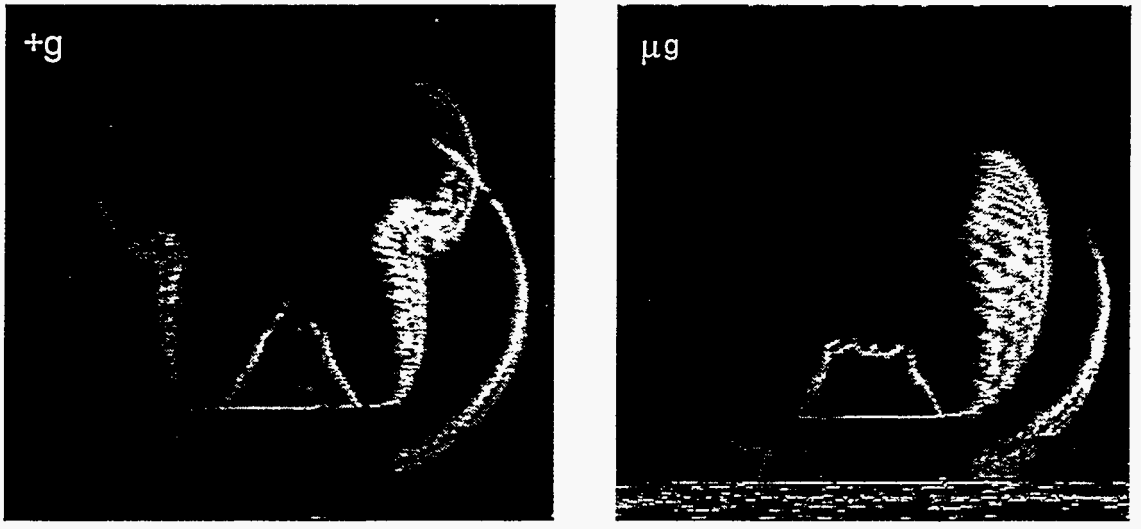

Figure 5 : Schlieren records of a laminar conical flame stabilized showing changes in flame shape from normal gravity (+g) to microgravity (µg).

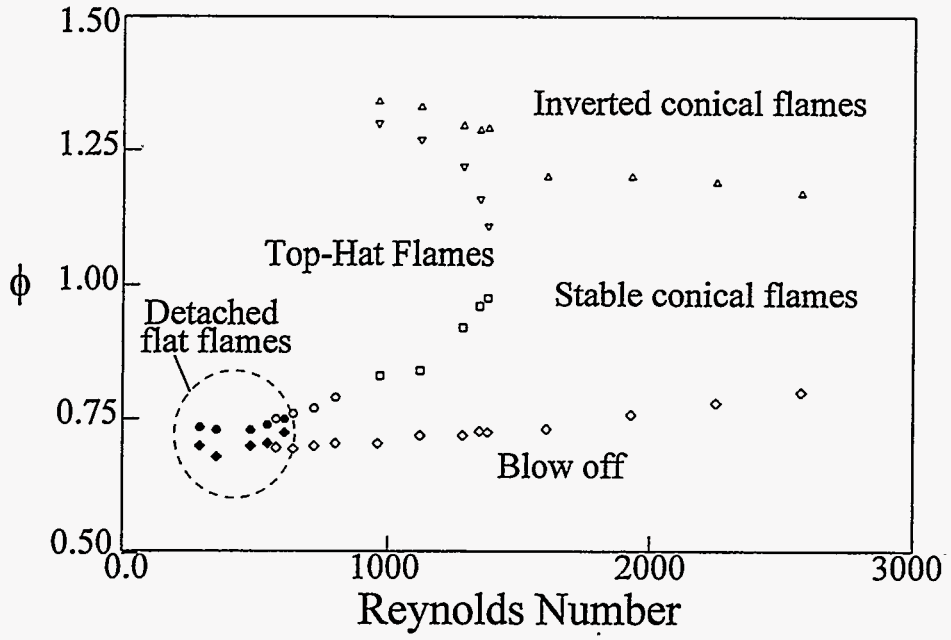

Figure 6 : Stabilization domain of the buoyancy stabilized laminar flat flame

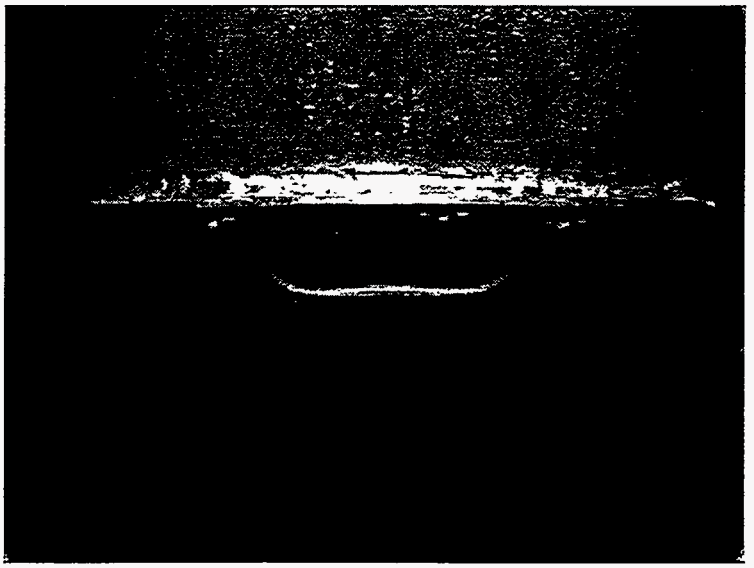

Figure 7 : Photograph of a buoyancy stabilized laminar flat flame.

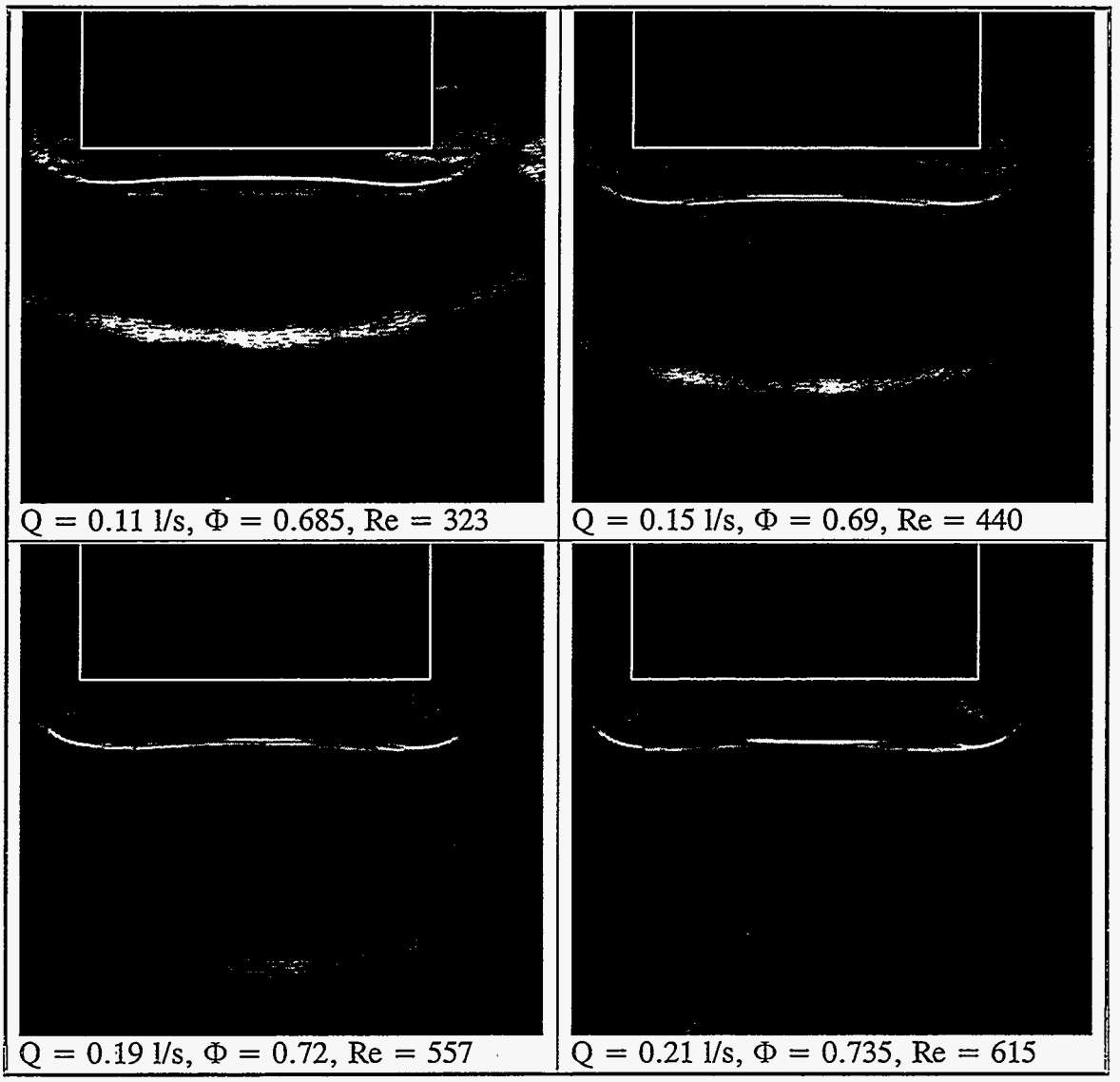

Figure 8 : Four schlieren images of stabilized laminar flat flames a increasing *Re*.

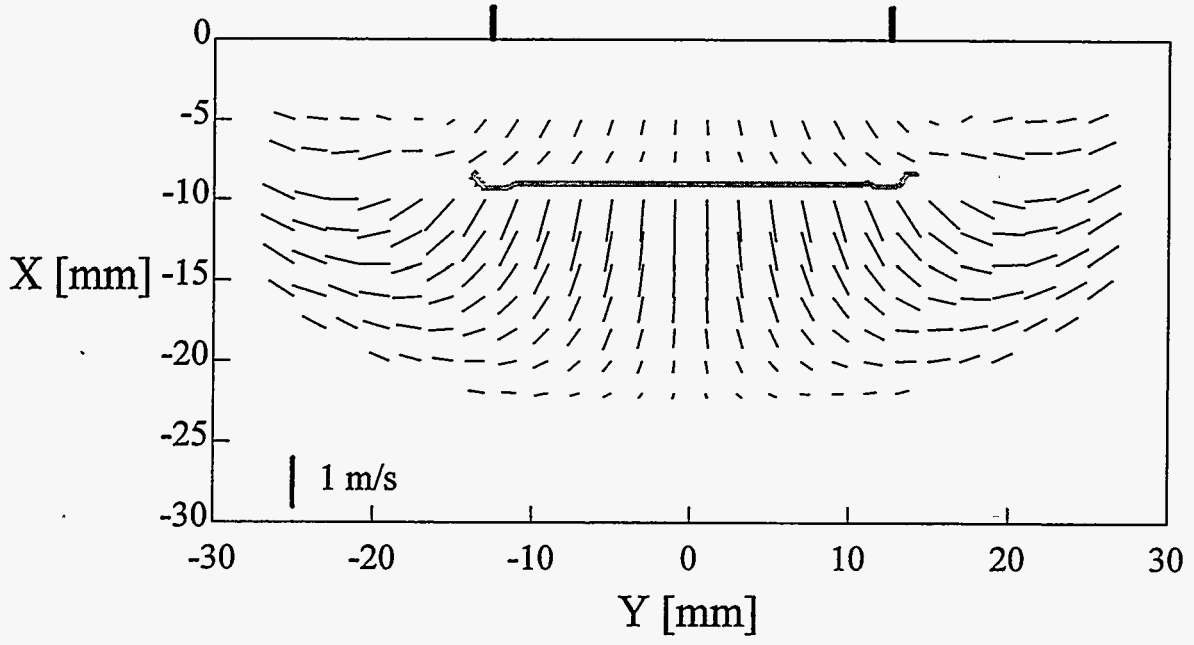

Figure 9 : Velocity vector measure in a buoyancy stabilized flame flame of $Q = 0.19$ l/s, $\phi = 0.735$

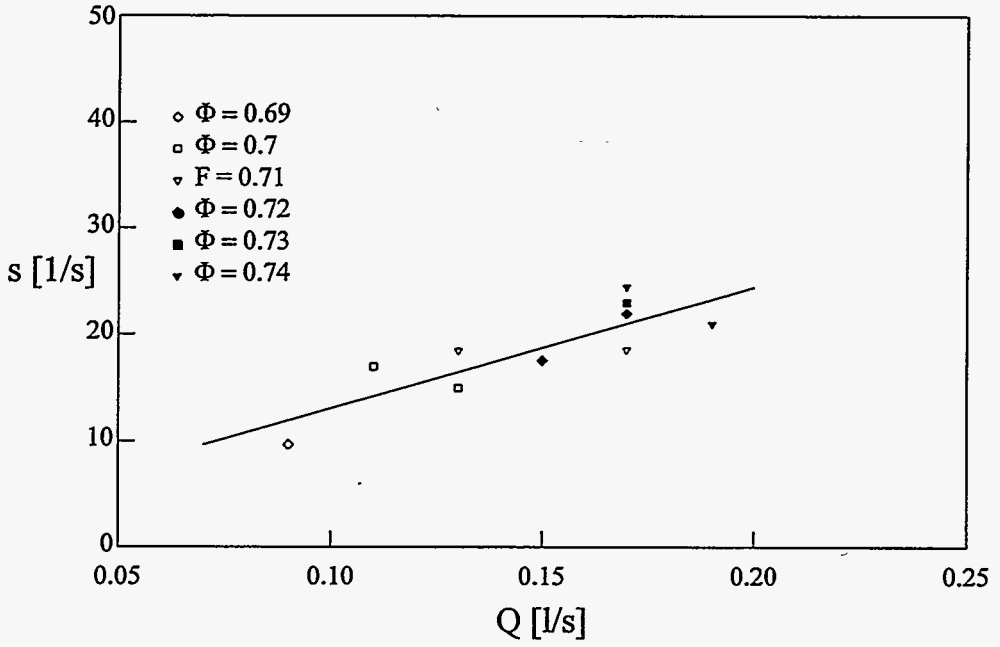

Figure 10 : Stretch rate, a, determined for cases listed in Table I.

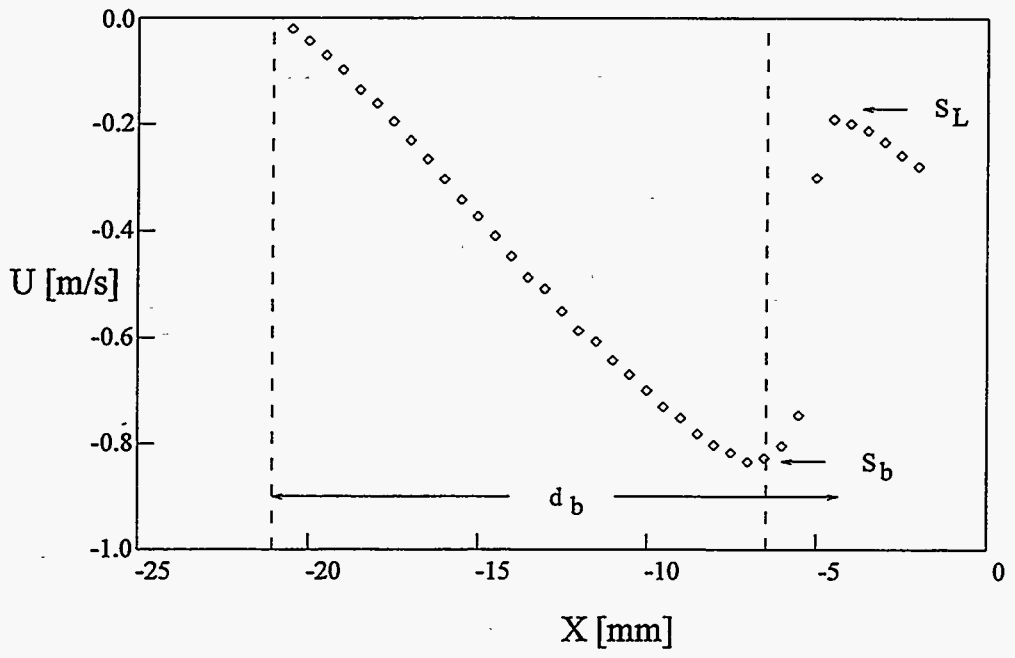

Figure 11 : Centerline velocity profile of a buoyancy stabilized flat flame with $Q = 0.17$, $\phi = 0.72$

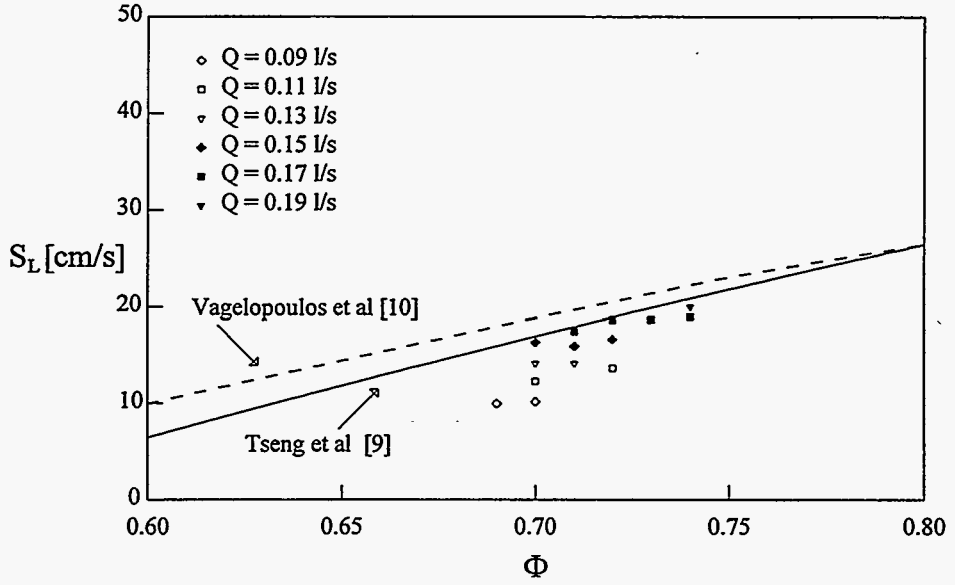

Figure 12 : Laminar flame speed, S_L determined for cases listed in Table I.

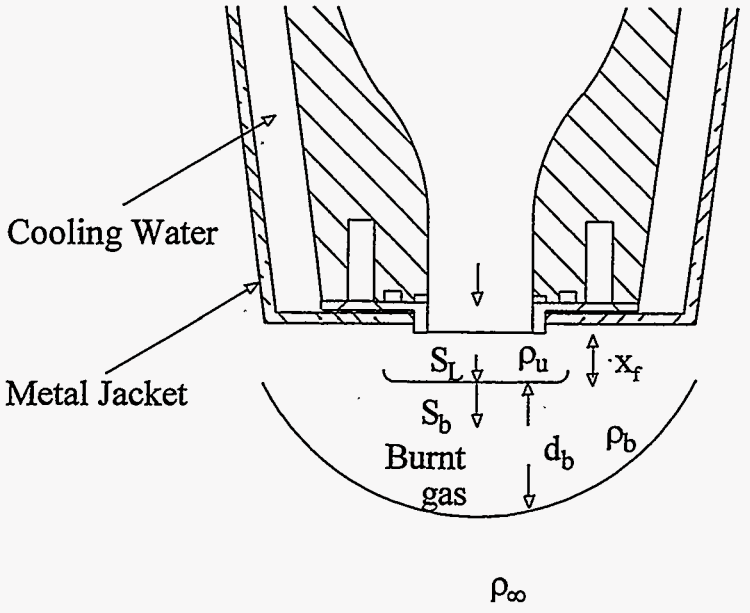

Figure 13 : Schematics of the flowfield generated by buoyancy stabilized flat flames.

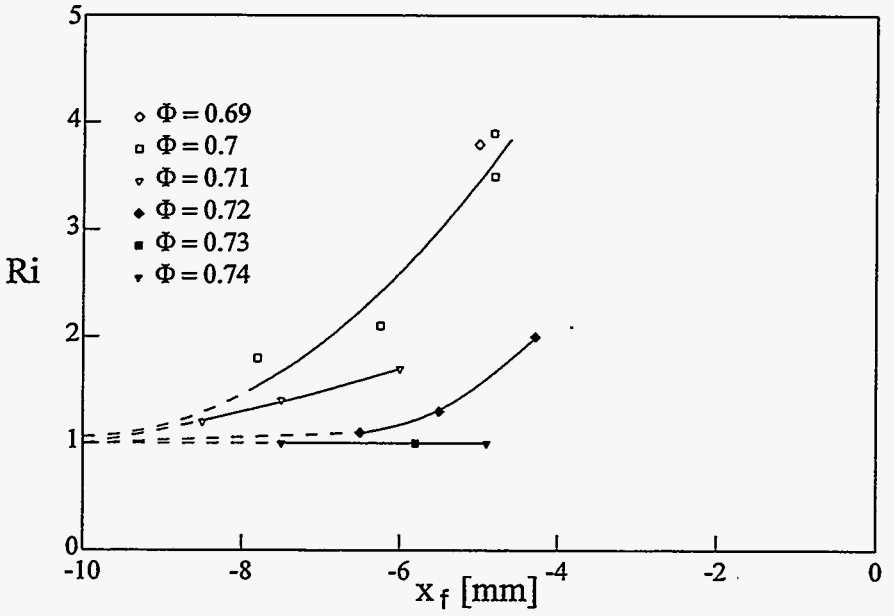

Figure 14 : Richardson number, *Ri*, determined for cases of Table I according to Equation (4).

LAWRENCE BERKELEY LABORATORY
UNIVERSITY OF CALIFORNIA
TECHNICAL AND ELECTRONIC
INFORMATION DEPARTMENT
BERKELEY, CALIFORNIA 94720